Quaternary Science Reviews 344 (2024) 108947

Contents lists available at ScienceDirect

Quaternary Science Reviews

journal homepage: www.elsevier.com/locate/quascirev

Hydroclimatic change and vegetation response in Tropical African alpine environments over the Holocene

Andrea Mason [a,b,*], James Russell [a], Sloane Garelick [a], Sarah Ivory [c], Meredith Kelly [d], Bob Nakileza [e], Nathan Anderson [d]

[a] Earth, Environmental, and Planetary Sciences Department, Brown University, Providence, RI, USA
[b] Institue at Brown for Environment and Society, Brown University, Providence, RI, USA
[c] Department of Geosciences and the Earth and Environmental Systems Institute, The Pennsylvania State University, University Park, PA, USA
[d] Department of Earth Science, Dartmouth College, Hanover, NH, USA
[e] Mountain Resource Centre, Makerere University, Kampala, Uganda

ARTICLE INFO

Handling editor: P Rioual

Keywords:
Africa
Organic geochemistry
Holocene
Paleoclimatology
Vegetation

ABSTRACT

Future precipitation is highly uncertain, particularly in East Africa where model projections contradict modern observational trends. Climate changes in East Africa's mountains are even less well understood, yet these mountains are threatened by warming, extreme flooding, fires, and the rapid disappearance of glaciers. Paleoclimatic and paleoenvironmental records can contextualize ongoing and future changes; however, proxy records from East African mountains disagree with each other and, in some cases, differ from nearby lowland sites. It is unclear if these discrepancies are due to geographic or altitudinal gradients in climate or processes that impact the fidelity of climate proxies in these mountains. To better understand past mountain precipitation and vegetation change, we produced three new records of the hydrogen and carbon isotopic composition of terrestrial leaf waxes (δ^2H_{wax} and $\delta^{13}C_{wax}$) spanning the Holocene using lake sediment cores collected from Lake Mahoma (2990 m asl), Lake Africa (3895 m asl), and Lake Kopello (4017 m asl) in the Rwenzori Mountains, Uganda-Democratic Republic of Congo. We find similar trends at all three sites in reconstructed precipitation hydrogen isotopic composition (δ^2H_{precip}), which we interpret to reflect precipitation amount. Our records show drying occurred during the Younger Dryas (~12 cal ka BP), enhanced precipitation during the African Humid Period (~10-5 cal ka BP) and drying in the mid to late Holocene (~5-0 cal ka BP), similar to adjacent lowland sites. We observe a gradual termination of the African Humid Period in the Rwenzori, consistent with many regional records. We also observe distinct patterns of Holocene precipitation change in Eastern and Western Africa, indicating differences in the delivery of moisture from the Atlantic and Indian Oceans. Despite changes in precipitation over the Holocene, the carbon isotopic composition of the waxes in Rwenzori lakes indicates constant C_3 vegetation and eco-hydrological stability, in contrast to sites from lower elevations. This likely indicates climate remained humid and cool enough throughout the Holocene to maintain forest and alpine plant communities at these high-elevation mountain sites.

1. Introduction

Future precipitation in Africa is poorly constrained, with model projections showing uncertainty in both the sign and magnitude of future precipitation in many parts of the continent (Niang et al., 2014; Trisos et al., 2022). This uncertainty is particularly acute in Africa's mountainous regions, where instrumental observations are extremely scarce and model resolution is too low to accurately capture the influence of topography on precipitation (Van Vooren et al., 2019). Qualitative observations from some tropical African mountains suggest that the frequency and intensity of precipitation events are increasing (Taylor et al., 2009; Bwambale et al., 2018), but with virtually no continuous instrumental records of precipitation it is difficult to assess patterns of change over time and whether current and future changes may threaten alpine ecosystems and the services they provide.

Paleoclimate records can supplement our understanding of climate change and ecosystem responses. However, paleoclimate records from tropical East African mountains are sparse and often in disagreement,

* Corresponding author. Earth, Environmental, And Planetary Sciences Department, Brown University, Providence, RI, USA.
E-mail address: andrea_mason@brown.edu (A. Mason).

https://doi.org/10.1016/j.quascirev.2024.108947
Received 28 May 2024; Received in revised form 30 August 2024; Accepted 3 September 2024
Available online 26 September 2024

possibly due to geographic or altitudinal gradients or local processes that could impact the fidelity of climate proxies in these mountains. For instance, despite their proximity, records from the mountains of Tanzania and Kenya diverge in their long-term hydroclimate trends and their proposed responses to climate forcing (e.g. Thompson et al., 2002; Garelick et al., 2021; Barker et al., 2001). High-elevation pollen records from the Rwenzori Mountains, Uganda-Democratic Republic of Congo show transitions in forest community assemblages over the Holocene, potentially in response to temperature and precipitation changes (Livingstone, 1967; Garelick et al., 2021), but these palynological records are not supported by independent estimates of precipitation change. Similar issues of proxy disagreement confound interpretation of records available from Mt. Kenya (Street-Perrott et al., 2007; Garelick et al., 2021; Barker et al., 2001). Thus, we are poorly equipped to examine the resilience and sensitivity of alpine vegetation to changing hydroclimate in East African mountains as well as the mechanisms governing long-term changes in precipitation.

African precipitation varied dramatically over the Holocene. The most pronounced change was during the African Humid Period (AHP) when increased northern hemisphere summer insolation strengthened the summer monsoon, giving rise to a "Green Sahara" in North Africa from approximately 14.8 to 5.5 ka (De Menocal et al., 2000). During this time, enhanced precipitation transformed the Sahara Desert into a vegetated landscape with large endorheic lakes (De Menocal, 2015; Shanahan et al., 2015; Tierney et al., 2017; De Menocal, 2015). However, records show variable timings and rates of the AHP termination across Africa, suggesting different mechanisms regulate regional precipitation. The timing of AHP termination is thought to have occurred earliest in Northern Africa where AHP termination occurred gradually at some sites but abruptly in others, where precipitation declined much faster than the change in insolation (De Menocal et al., 2000; Schefuβ et al., 2005; Shanahan et al., 2015; Tierney et al., 2017). Whereas seasonal insolation forcing of the North African monsoon coupled with land-surface feedbacks could explain the AHP and its rapid termination in North Africa (De Menocal et al., 2000; Liu et al., 2006), it is now widely recognized that precipitation increased over much of northern Africa as well as equatorial Africa as far south as Lake Tanganyika during the AHP (6° S, Otto-Bliesner et al., 2014), which cannot easily be explained by insolation forcing nor vegetation feedbacks (Costa et al., 2014; Tierney et al., 2011a, 2011b). The rate of AHP termination is also inconsistent across East Africa. Some sites, such as Lake Tanganyika and Lake Chala (Tierney et al., 2008, 2011b) show abrupt terminations similar to records from North Africa (Castañeda et al., 2016; Niedermeyer et al., 2010; Tierney et al., 2017), whereas records from Lake Victoria and Lake Rutundu show a gradual AHP termination, more similar to the rate of change in North African summer insolation forcing despite their equatorial location (Berke et al., 2012; Garelick et al., 2021). The inconsistencies among East African hydroclimate records confounds our understanding of how regional hydroclimate forcings and dynamics result in varying AHP responses across East Africa.

To improve our understanding of tropical East African montane hydroclimate, we present new hydrogen and carbon isotope records from terrestrial leaf waxes (δ^2H_{wax} and $\delta^{13}C_{wax}$) from three lakes in the Rwenzori Mountains, Uganda-D.R.C. These are the highest-elevation biomarker records of hydroclimate and vegetation from Africa providing a unique insight into Afro-montane climate and environmental dynamics. We compare our records to other leaf wax isotope records from high-elevation East African mountains to advance the understanding of the climate-vegetation relationship in Afro-alpine environments and to evaluate how AHP dynamics in the Rwenzori differ from elsewhere in Africa. These data reveal the sensitivity of montane precipitation to changing boundary conditions and the impacts of changing climate on vegetation composition.

2. Study site

The Rwenzori Mountains, the third tallest mountain range in Africa (5109 m asl), are an uplifted horst block along the western arm of the East African Rift that straddles the Uganda-Democratic Republic of Congo border (Fig. 1) (Russell et al., 2009; Taylor et al., 2009). They are one of three currently glaciated mountain ranges in Africa, in addition to Mt. Kilimanjaro and Mt. Kenya. Among these, the Rwenzori contains the largest number of glaciers and most expansive Afro-alpine ecosystem in Africa (Livingstone, 1967; Osmaston, 1989; Kaser and Osmaston, 2002).

Western Uganda sits within a transition zone between the wet climate of Central Africa, which supports the Guineo-Congolian rainforest, and the drier climate and savannahs of East Africa (Diem et al., 2019). The altitudinal range of the Rwenzori hosts rich floral biodiversity across four main vegetation zones: the montane forest zone (~1800–2400 m asl), the bamboo zone (~2400–3000 m asl), the ericaceous belt (~2700–3900 m asl), and the alpine belt (>3800 m asl) (Livingstone, 1967). The alpine belt is home to distinctive endemic plants including *Lobelia* and *Dendrosenecio*. The diversity of ecosystems in the Rwenzori Mountains has also promoted faunal biodiversity, cementing its status as a national park, a UNESCO world heritage site, and a conservation priority.

Ugandan precipitation is impacted by the north-south seasonal migration of the Intertropical Convergence Zone (ITCZ) across the equator which results in a bimodal precipitation regime (Nicholson, 2017). Additionally, the region is also influenced by the southeast-northwest movement of the Congo Air Boundary (CAB) (Taylor et al., 2009; Tierney et al., 2011a, 2011b), a convergence zone between unstable moist air from the Congo Basin and drier air from the Indian Ocean. Eastward migration of the CAB can promote incursions of moist, unstable air masses from the Atlantic into eastern Africa (Nicholson, 2017). In the Rwenzori Mountains the two rainy seasons are from March to May and from August to November, although precipitation at higher elevations occurs year-round. The Rwenzori receive an average of 2500 mm of precipitation a year at high elevations due to orographic effects and its location in the climate transition zone (Russell et al., 2009; Osmaston, 1989).

3. Methods

3.1. Sample collection

Multiple cores were recovered from three different lakes in the Rwenzori Mountains. Two cores were recovered from Lake Mahoma, located at 2990 m asl (core MAHO08: coordinates 0.34 °N, 29.96 °E, water depth 11.8 m; core MAHO19: coordinates 0.34 °N, 29.96 °E, water depth 11.5 m) (Garelick et al., 2022). One core was recovered from Lake Africa, located at 3895 m asl (core LAFR19, coordinates 0.29 °N, 29.89 °E, water depth 4.5 m), and one core from Lake Kopello, located upstream from Lake Africa, at 4017 m asl (core LKOP19, coordinates 0.31 °N, 29.89 °E, water depth 11 m). These lake sediment cores were obtained using a modified Livingstone square-rod piston corer and winch-operated tower deployed from a raft in January 2019. Meter-long core sections were taken from overlapping holes until penetration became impossible due to coarse sands and pebbles. Multiple cores were taken from adjacent holes to obtain overlapping core sections for the entirety of the sediment depth. Cores were extruded on site and sealed for transport in polyethylene sleeves contained within polyvinyl chloride tubes. The uppermost sediment sequences were obtained for Lake Mahoma from an additional shallow core collected in January 2008 using a Bolivia corer (Garelick et al., 2022).

All cores were split, imaged, and scanned for magnetic susceptibility on a GeoTek multi-sensor core logger at 1-cm resolution at Brown University and were visually described using the strategies described in Schnurrenberger et al. (2003). Composite stratigraphies were made for Lake Kopello and Lake Africa by cross-correlating shared features in the

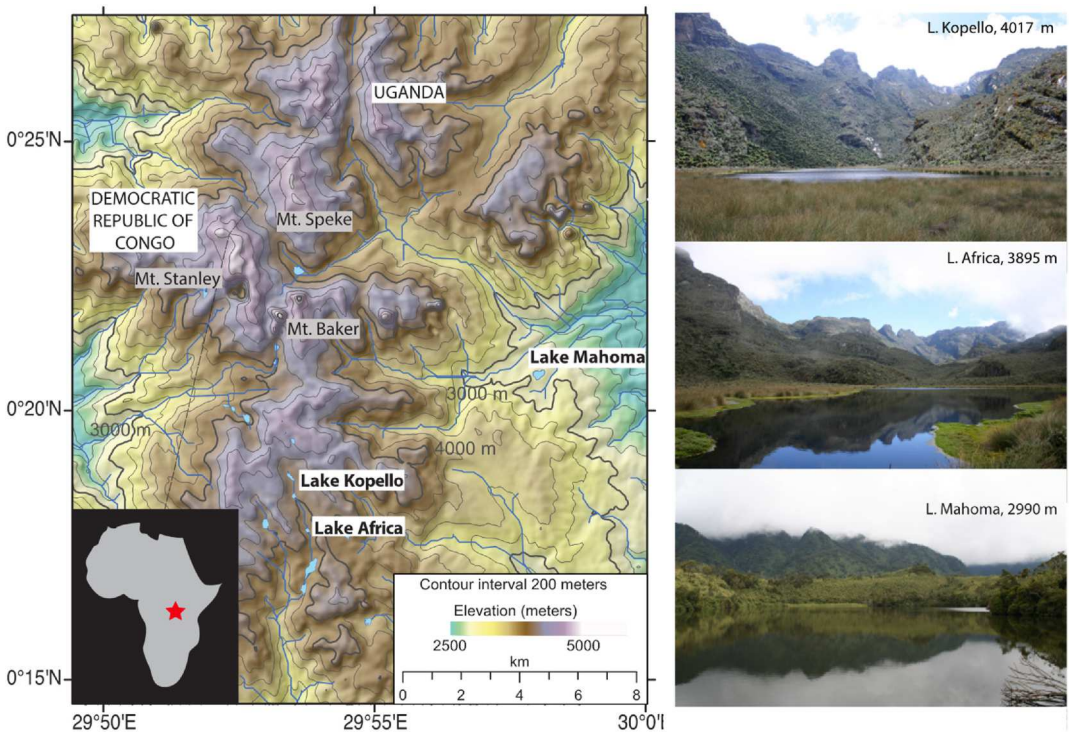

Fig. 1. A map of Africa with the location of the Rwenzori Mountains (red star) and a regional topographic map with the locations of Lake Mahoma, Lake Africa, and Lake Kopello. Images (right) show Lake Kopello (4017 m), Lake Africa (3895 m), and Lake Mahoma (2990 m).

visual stratigraphy and in magnetic susceptibility. A previous stratigraphic composite section was created by Garelick et al. (2022) for Lake Mahoma.

3.2. Age-depth model

To develop age-depth models for these cores, 14 samples of bulk sediment from Lake Africa (Supplemental Table 1) and 16 bulk sediment samples from Lake Kopello (Supplemental Table 2) were radiocarbon dated by accelerator mass spectrometry (AMS) at the National Ocean Sciences AMS (NOSAMS) facility at the Woods Hole Oceanographic Institution. Radiocarbon ages were calibrated using CALIB8.2 (Stuiver and Reimer, 1993). Using the R package *geoChronR*, we created age model ensembles for each lake using the packages *bacon*, *Bchron*, and Oxcal calibrated using IntCal20 (McKay et al., 2021, Reimer et al., 2020). The ensemble for each lake consists of 1000 iterations per age model, totaling 3000 members for the grand ensemble. Although a Bayesian age model for Lake Mahoma was published previously, we created a new age model ensemble for consistency using 16 previously published radiocarbon ages from the site (Garelick et al., 2022) (Fig. 2).

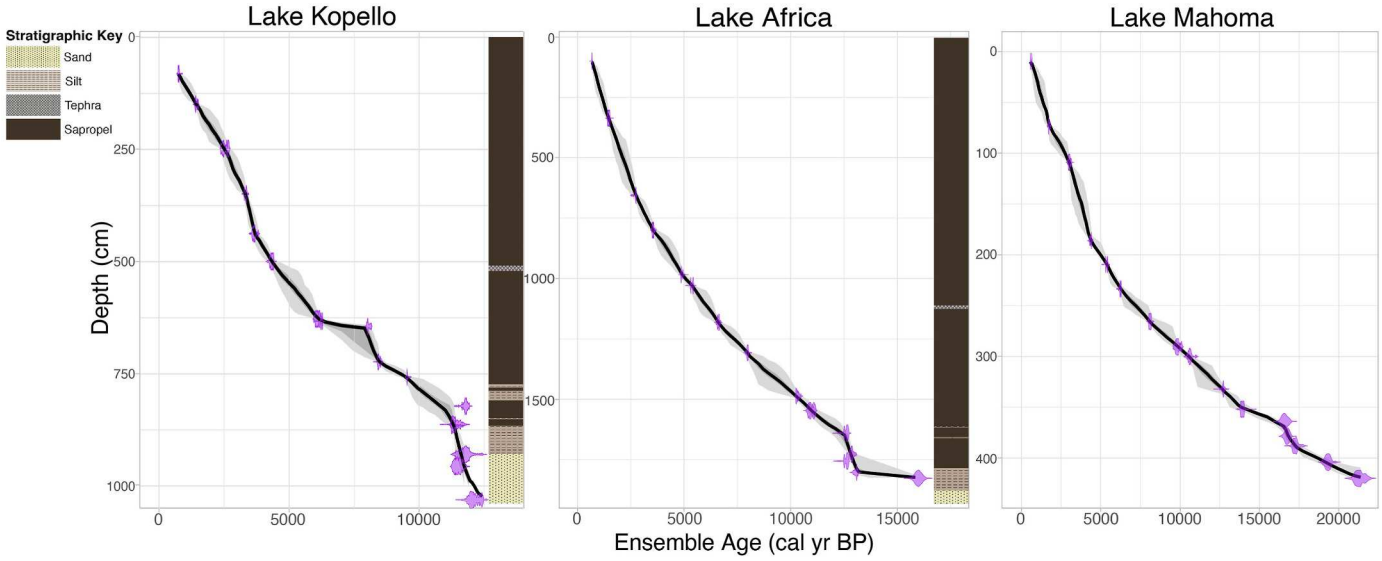

Fig. 2. *GeoChronR* (Mckay et al., 2021) age model ensembles for Lake Kopello, Lake Africa, and Lake Mahoma. Relative age probability distributions are in purple, black line is median age, dark gray shading is 50th percentile probability range, light gray shading is 95th percentile probability range. Stratigraphic columns are included for Lake Kopello and Lake Africa and a detailed stratigraphy, as well as a table of radiocarbon ages for Lake Mahoma are found in Garelick et al. (2022).

3.3. Sample preparation and analysis

We subsampled the sediment cores in 2 cm sections at an average resolution of 19 cm in Lake Kopello (n = 44) and an average resolution of 40 cm in Lake Africa (n = 44). From Lake Mahoma cores, we subsampled the core in 1 cm sections at an average resolution of 5 cm (n = 56). From the sediment samples, we measured the carbon and hydrogen isotopic composition of terrestrial leaf waxes, specifically long-chain *n*-alkanes, to reconstruct past precipitation and vegetation isotope composition. Long-chain (C_{29}-C_{33}) *n*-alkanes are synthesized by terrestrial plants, transported by eolian and fluvial process into lakes, and preserved in lake sediments. To isolate *n*-alkanes from the sediment, 0.5–2 g samples were taken from cleaned core surfaces, freeze-dried, and soluble lipids were extracted using 9:1 dichloromethane:methanol (DCM:MeOH) in a DIONEX Accelerated Solvent Extractor 350 to produce a total lipid extract (TLE). 10–20 mg of TLE from each sample was separated into neutral and acid fractions using an aminopropyl column separation with DCM:isopropoanol (2:1) and ether:acetic acid (24:1). The neutral fraction containing n-alkanes was further separated by polarity on an alumina column using hexane, DCM, 1:1 DCM:MeOH, and MeOH as eluents. The hexane fraction was further purified using a silver nitrate column to separate saturated and unsaturated hydrocarbons using hexane followed by ethyl acetate. Relative concentrations of saturated *n*-alkanes were quantified using an Agilent 6890 gas chromatograph (GC) with an HP1-MS column (30 m × 0.25 mm × 0.25 μm) and flame ionization detector (FID).

Following quantification, we measured the hydrogen (δ^2H) and carbon ($\delta^{13}C$) isotopic compositions of the C_{29} and C_{31} n-alkanes, focusing on C_{31}. We measured C_{31} alkane δ^2H (δ^2H_{C31}) and $\delta^{13}C$ values ($\delta^{13}C_{C31}$) using an Agilent 6890 GC equipped with a ZB5-MS plus column (30 m × 0.32 mm × 0.25 μm) coupled to a Thermo Delta V Plus isotope ratio mass spectrometer. The oven program was as follows: an initial temperature of 40 °C and hold for 1 min, increase to 230 °C at 15 °C/min, then increase to 320 °C at 10 °C/min and hold for 10 min. H^{+3} factors (Sessions et al., 2001), measured at least every 3 days, averaged 2.00 ± 0.05 (1σ). An *n*-alkane standard mixture consisting of alkanes of known isotopic composition from Schimmelmann Labs (δ^2H_{C29} = −162.6 ± 2.2‰; δ^2H_{C31} = −271.9 ± 2.0‰; δ^2H_{C32} = −212.4 ± 1.0‰; $\delta^{13}C_{C29}$ = −29.30 ± 0.02‰; $\delta^{13}C_{C31}$ = −29.43 ± 0.01‰; $\delta^{13}C_{C32}$ = −29.47 ± 0.02‰) was injected after every nine δ^2H and $\delta^{13}C$ measurements. The mean difference between bracketing measured and reported values was applied to measured δ^2H_{C31} values to correct for instrument offset and drift. Using methods described by Mitsunaga et al. (2023), we estimated δ^2H_{precip} by applying the apparent fractionation between δ^2H_{precip} and δ^2H_{wax} using a vegetation correction that utilizes $\delta^{13}C_{wax}$ to define the abundance ratio between C_3 and C_4 plant waxes at each lake. We use the apparent fractionation of C_{27} *n*-alkanes for C_3 and C_4 plants, −128.9‰ and −125.4‰, identified by Konecky et al. (2016) as the average end-members for tropical vegetation (i.e., between 30° N and 30° S). Additionally, we employ the fraction of C_3 and C_4 plants contributing leaf waxes to each sample, calculated using the linear mixing model described by Uno et al. (2016). We used the *n*-alkane end-member values specific for East Africa proposed by Uno et al. (2016), which are −31.1‰ for C_3 and −19‰ for C_4. For our correction we used $\delta^{13}C_{wax}$ values from each respective core, which we interpolated to our time series of δ^2H_{wax}.

4. Results

4.1. Sediment stratigraphies and ages

The succession from Lake Kopello consists of ~9.7 m of sediment spanning the last 12.5 kyr. The basal sediments consist of ~1.2 m of light gray to brown thin-to medium (~0.5–10 cm) bedded sands and silts that gradually grade into a massive, dark brown to black silty sapropel. Two medium beds of coarse silt are present at ~7.7 and 7.9 m depth. A tephra, previously identified in sediments from Lake Mahoma (Livingstone, 1967; Garelick et al., 2022) occurs at ~5.1 m depth. Radiocarbon ages indicate very rapid sedimentation rates in the basal sands and silts, and relatively constant and slower sedimentation rates in the sapropel. Overall, we interpret this succession to reflect rapid inputs of clastic sediment following deglaciation of the lake basin by ~12.5 cal ka BP, followed by establishment of a lake ecosystem more similar to the present day.

The succession from Lake Africa consists of 17.7 m of sediment spanning the last 13.6 kyr. The slightly older basal age for Lake Africa relative to Kopello is consistent with upslope glacial retreat from Lake Africa's downstream position in the Nyamugasani catchment. Overall, the stratigraphy is similar to that from Lake Africa, with ~1.2 m of thinly-to medium bedded light gray to brown thin-to medium bedded sands and silts grading upward into a massive, dark brown to black silty sapropel. The tephra observed in Lake Africa is present at 10.2 m depth.

Our age models indicate the stratigraphic successions from Lakes Kopello, Africa, and Mahoma span the last 12.5, 13.6, and 21.3 kyr, respectively. Sedimentation rates in Lakes Kopello, Africa, and Mahoma average 0.77 (min: 0.10, max: 2.58), 1.31 (min: 0.01, max: 1.16), and 0.27 m/kyr (min: 0.11, max: 0.60), respectively. The source and age of the tephra are unknown (Livingstone, 1967); however, our age models predict the ages of the tephra, which is observed in all successions, is ~5.43 cal ka BP (97.5% CI [4.82–5.92]) in Lake Kopello, 5.35 cal ka BP (97.5% CI [5.19–5.44]) in Lake Africa, and 5.42 cal ka BP (97.5% CI [5.19–5.58]) in Lake Mahoma. The similarity of tephra ages amongst all three lakes demonstrates the consistency of our age models.

4.2. Leaf wax distributions and isotopic compositions

Sediment *n*-alkane distributions were summarized using Average Chain Length (ACL; calculated as in Castañeda et al., 2016). We found ACL values between 28 and 31 in Lake Kopello, between 27 and 29 in Lake Africa, and 28 and 32 in Lake Mahoma (Supplemental Fig. 2). We also calculated the Carbon Preference Index (CPI; Bray and Evans, 1961), which quantifies the relative abundances of odd to even chain length *n*-alkanes to evaluate degradation of the waxes. Petroleum sources have CPI values of 1, and higher plants have CPI values above 3. We found ACL values between 5 and 14 in Lake Kopello, between 6 and 12 in Lake Africa, and between 5 and 14 in Lake Mahoma, indicating excellent preservation of the waxes (Supplemental Fig. 2). Neither CPI nor ACL correlated with respective isotope timeseries at any site, which indicates variations in leaf wax source and degradation have limited impacts on the isotopic values (Supplemental Fig. 2).

The isotopic compositions of different *n*-alkanes within Lakes Mahoma, Kopello, and Africa are strongly correlated (Supplemental Figs. 4, 5, 6). In particular, the δ^2H_{C31} values are all characterized by depleted values in the early Holocene, and more enriched values in the late Holocene, with generally strong and significant correlations (Supplemental Figs. 4, 5, and 6). We use the δ^2H of C_{31} (δ^2H_{C31}) to represent these compositions in Lake Africa, Lake Kopello, and Lake Mahoma, as the δ^2H_{C31} was most consistent across the sites. The δ^2H_{wax} average sampling resolution in Lake Mahoma was 0.205 kyr and values ranged from −107‰ to −169‰, with more depleted values in the early Holocene relative to the late Holocene (Fig. 3). Lake Kopello δ^2H_{wax} average sampling resolution was 0.245 kyr and values ranged from −142 to −172‰. Lake Africa δ^2H_{wax} average sampling resolution was 0.286 kyr and values ranged from −145 to −183‰. Both these lakes show similar trends to Lake Mahoma, but with a lower-amplitude transition from the early to the late Holocene. Near-modern δ^2H_{wax} values from Kopello and Africa are more depleted than those observed at Lake Mahoma, in keeping with isotopic depletion of precipitation at higher elevations (~4000 m asl at Kopello and Mahoma, 3000 m at Lake Mahoma) (Garelick et al., 2021). The δ^2H_{wax} records at Lakes Kopello and Africa are also very similar to each other, consistent with their proximity.

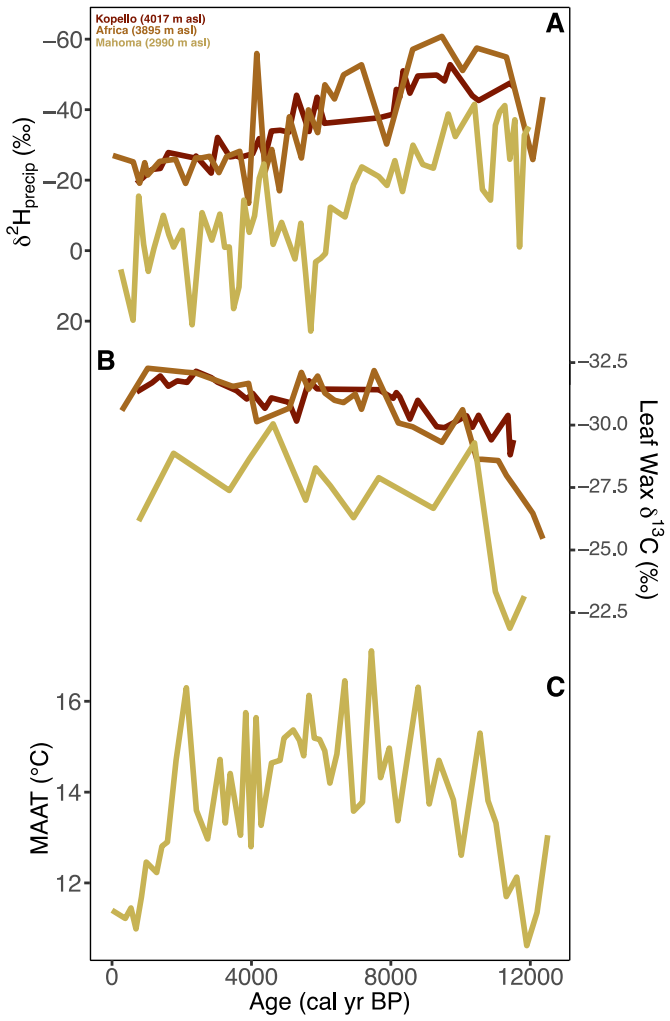

Fig. 3. A. Holocene leaf wax records of δ^2H_{precip} from the Rwenzori indicate precipitation intensified in the early Holocene and gradually reduced throughout the middle to late Holocene. B. Leaf wax $\delta^{13}C_{wax}$ values from high elevation Rwenzori lakes (Lake Africa and Lake Kopelllo) show isotopic compositions generally consistent with C_3 vegetation despite changes in climate (δ^2H_{precip} and MAAT), whereas middle elevation Lake Mahoma $\delta^{13}C_{wax}$ demonstrates more isotopic variability consistent with changes in C_3 versus C_4 abundance. C. Lake Mahoma Holocene br-GDGT mean annual air temperature (MAAT) record (Garelick et al., 2022) shows peak warming over the middle Holocene.

The $\delta^{13}C_{wax}$ in Lakes Kopello and Africa exhibit nearly identical trends over the last 12 kyr. Their $\delta^{13}C_{wax}$ is relatively enriched during the latest Pleistocene, exhibiting values between −27‰ and −29‰–11.5 cal ka BP, followed by a gradual trend of ^{13}C depletion of −2 to −4‰ over the Holocene (Fig. 3). The Lake Mahoma $\delta^{13}C_{wax}$ values are more enriched relative to the higher-elevation lakes, with a maximum of −21‰ in the late Pleistocene and values between −26 and −29‰ throughout the Holocene, suggesting that Lake Mahoma receives more wax from plants using the C_4 photosynthetic pathway. The $\delta^{13}C_{wax}$ in Lake Mahoma were measured at lower resolution and more variable than in the other lakes but generally exhibit the same trends. Correcting the δ^2H_{wax} values for vegetation composition based on $\delta^{13}C_{wax}$ adjusts the mean of δ^2H_{precip} values but has little impact on the trends in each record (Supplemental Fig. 3).

5. Discussion

5.1. Precipitation isotope records from tropical African mountains

In high-elevation regions such as the Rwenzori, the isotopic composition of precipitation can be impacted by vertical temperature changes and Rayleigh distillation whereby upslope isotope values are more depleted due to cooler temperatures and fractional distillation (Garelick et al., 2021; Rowley and Garzione, 2007). In the Rwenzori Mountains, we find in the late Holocene records from the highest elevation lakes, Lake Africa (3895 m asl) and Lake Kopello (4017 m asl), had more depleted δ^2H_{precip} values than mid-elevation Lake Mahoma (2990 m asl), as expected due to upslope Rayleigh distillation (Fig. 3). This observation, combined with the overall similarity in δ^2H_{precip} records at all three lakes, and particularly in Lakes Africa and Kopello, provides evidence for the reliability of leaf wax hydrogen isotope reconstructions in this environment.

In the tropics, where there is little seasonal temperature variation, precipitation amount is the dominant control on precipitation isotopes (Bowen, 2008) although moisture source, transport, convection, and other atmospheric processes may also influence precipitation isotope compositions (Dansgaard, 1964; Konecky et al., 2019). The hydrogen isotopic composition of terrestrial plant waxes is strongly correlated to the mean annual precipitation δ^2H (δ^2H_{precip}) (Sachse et al., 2012), allowing us to infer precipitation amount. The so-called "amount effect" has been used to infer past precipitation in many African δ^2H records, wherein relative depletion of leaf wax hydrogen isotopes corresponds to an increase in precipitation and vice versa (Berke et al., 2012; Dansgaard, 1964; Sachse et al., 2012; Schefuβ et al., 2005; Tierney et al., 2008). Recent data-model syntheses suggest high-elevation precipitation isotope records could respond strongly to high-elevation temperatures due to Rayleigh distillation and thermodynamic processes in the middle to upper troposphere (Liu et al., 2023). However, temperatures in the Rwenzori from Lake Mahoma estimated from organic geochemical proxies show a climate history that is also reflected in pollen and moraine records (Garelick et al., 2022), but differs from trends in δ^2H_{precip}, indicating that temperature changes are not the dominant control on δ^2H_{precip} in this environment during the Holocene (Fig. 3). We therefore suggest that δ^2H_{precip} at these sites is primarily an indicator of changes in precipitation amount.

Prior research in East African mountains aimed to characterize their temperature and glacial history using a variety of geochemical, sedimentological, and palaeoecological indicators, but less is understood about these mountains' hydroclimate history (Doughty et al., 2023; Garelick et al., 2022; Russell et al., 2009; Taylor et al., 2009). Despite the proximity of existing high-elevation East Africa hydroclimate records, the climate histories inferred at high elevations often show differing trends. Leaf wax isotope records from Lake Rutundu on Mt. Kenya (3018 m asl) show enhanced precipitation in the AHP followed by a gradual drying trend which began around 9.7 cal ka BP (Garelick et al., 2021), similar to leaf wax isotopes from the Rwenzori (Fig. 4). In contrast, diatom oxygen isotope records from Small Hall Tarn (4289 m asl) and Simba Tarn (4595 m asl), also on Mt. Kenya, show isotopic minima about 9 cal ka BP and from 6.9 to 5.8 cal ka BP, interpreted to reflect intervals of enhanced precipitation (Fig. 4), interpreted to result from warm sea surface temperature anomalies in the Indian Ocean (Barker et al., 2001). Ice core oxygen isotope records from Mt. Kilimanjaro, Tanzania, show abrupt excursions at 8.3, 5.2, and 4 ka that are not reflected in other records (Fig. 4) (Thompson et al., 2002). Additionally, Thompson et al. (2002) suggest a late Holocene humid period occurred from 6.5-4.5 ka, which was less intense than the early Holocene humid period. The precise timing of these events is uncertain since the ice-core age model is not based on direct age measurements but rather on tuning the ice core $\delta^{18}O$ to a speleothem $\delta^{18}O$ record from Soreq Cave, Israel (Bar-Matthews et al., 1999). A δ^2H_{wax} record from Lake Chala, located on the eastern slope of Mt Kilimanjaro, does not show evidence for a

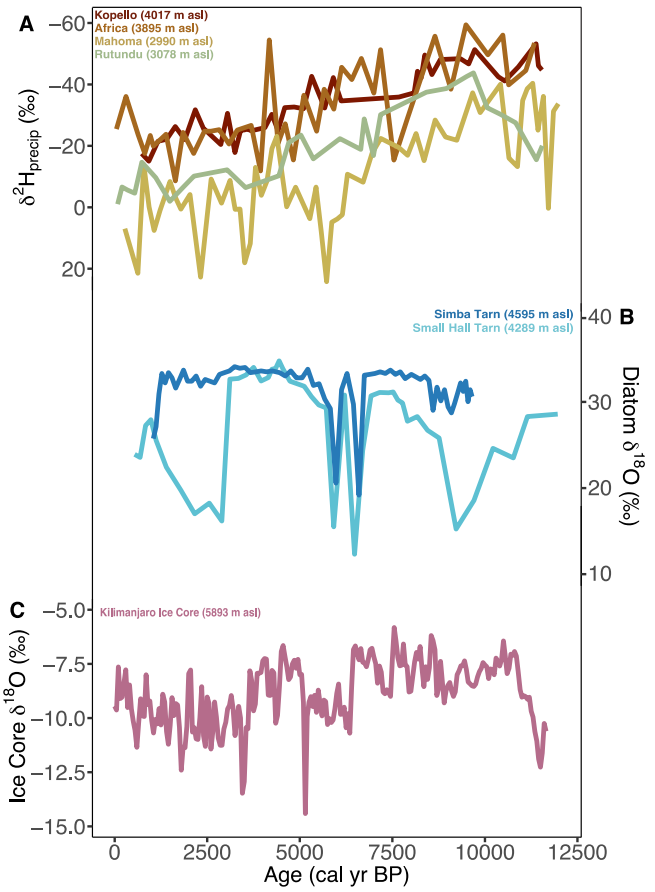

Fig. 4. A. Holocene East African mountain hydroclimate leaf wax δ^2H_{precip} records from Lake Kopello, Lake Africa, and Lake Mahoma (this study), Lake Rutundu (Garelick et al., 2021), B. diatom $\delta^{18}O$ records from Small Hall Tarn and Simba Tarn (Barker et al., 2001), and C. an ice core $\delta^{18}O$ record Mt Kilimanjaro (Thompson et al., 2002).

second humid period or a drought at 4 cal ka BP (Tierney et al., 2011b). However, the hydroclimatic interpretation of the Lake Chala record is difficult given two conflicting precipitation records exist. The δ^2H_{wax} record shows trends consistent with regional records of the AHP, whereas a branched and isoprenoid tetraether (BIT) index record suggests Holocene precipitation was driven by half-precession dynamics (Karp et al., 2023; Tierney et al., 2011a; Verschuren et al., 2009). The differences among high elevation hydroclimate records may arise because of real differences in precipitation in these topographically complex mountains, uncertainties in sediment- and ice-core chronologies, or uncertainties in the various precipitation proxies used in these studies. Whatever the case, the inconsistency between records in East Africa makes it difficult to understand the forcings and mechanisms driving precipitation change and their impacts on montane ecosystems.

Our three new leaf wax isotope records from lakes in the Rwenzori Mountains, two of which are the highest elevation leaf wax isotope records of hydroclimate in Africa, help to address these issues. We find δ^2H_{precip} trends over the Holocene which are consistent amongst the three lakes, and our age models predict nearly identical ages for a mid-Holocene tephra deposit which suggests the chronologies are consistent. Trends in our records are similar to those in a δ^2H_{precip} record from Lake Rutundu on Mt Kenya (Fig. 4); we observe an interval of ^2H-enriched waxes associated with the dry conditions coincident with the Younger Dryas (~11 cal ka BP), a rapid rebound to ^2H-depleted values and wetter conditions associated with the AHP (~10-6 cal ka BP) and drying during the mid-to late Holocene beginning around ~5 ka. The similarity of the δ^2H_{precip} records from these montane and alpine sites suggest that precipitation in these equatorial African mountains, separated by ~1000 km of longitude and 1000 m of elevation, experienced similar trends through the late Pleistocene and Holocene. Thus, when comparing the same proxy, isotopic records of precipitation agree with one another, which may suggest various other proxies record other aspects of hydroclimate.

Like the Rwenzori Mountains, many leaf wax records in East Africa exhibit drying during the YD including lowland sites such as Lake Albert and Lake Victoria (Berke et al., 2012, 2014). These observations confirm that precipitation in the high-elevation regions of equatorial East Africa is also sensitive to climatic teleconnections associated with high-latitude meltwater discharge and reductions in the Atlantic Meridional Overturning Circulation (AMOC). This is likely consistent with southward shifts in the Intertropical Convergence Zone in response to the reduction in northward ocean heat transport and northern high latitude cooling (Berke et al., 2014; Costa et al., 2014).

Following the YD, precipitation increased rapidly in the Rwenzori at the start of the African Humid period at ~11.5 ka, followed by drying beginning about 9 ka. In the Rwenzori montane records, the transition from a wet AHP to a dry late Holocene was gradual, occurring over millennia (Fig. 4). This sequence is also observed in core stratigraphic and geochemical changes in nearby lowland Lake Edward (Russell et al., 2003) as well as Lake Rutundu (Garelick et al., 2021), which implies that mountain environments in East Africa responded to the same large-scale forcings and circulation patterns influencing regional hydroclimate variability.

5.2. *Ecosystem stability in the Rwenzori Mountains*

Changes in temperature, precipitation and its seasonality, and atmospheric CO_2 concentrations influence the abundance of C_3 and C_4 vegetation on landscapes (Cerling et al., 1993). Because C_4 plants are able to concentrate CO_2 in their bundle sheath cells, they are best adapted to low CO_2 climates (Ehleringer et al., 1997). Temperature is another primary driver of vegetation distribution, with high growing season temperatures favoring C_4 vegetation (Ehleringer et al., 1997; Garelick et al., 2022). Lastly, a drier climate, particularly a longer dry season, favors C_4 grasses relative to most trees and shrubs that use the C_3 photosynthetic pathway (Garelick et al., 2022; Ehleringer et al., 1997; Cerling et al., 1993). Today, high-elevation Rwenzori ecosystems are dominated by C_3 vegetation (Garelick et al., 2022; Oyana and Nakileza, 2016; Livingstone and Clayton, 1980). Whereas leaf-wax isotope records from Mt. Kenya suggest variable abundances of C_4 plants during the late Pleistocene and Holocene (Huang et al., 1999; Garelick et al., 2021), potentially due to changes in atmospheric CO_2 concentrations and/or precipitation, similar records do not exist from the Rwenzori or most other tropical African mountains.

To understand the influence of changing climate on afro-montane vegetation, we analyzed the $\delta^{13}C$ of leaf waxes over the latest Pleistocene and Holocene. At high-elevation Lake Kopello and Lake Africa, $\delta^{13}C_{wax}$ values remained stable and within the range of tropical C_3 vegetation ($\delta^{13}C$ endmember for East Africa −31.1‰; Uno et al., 2016) throughout much of the Holocene, indicating no major changes in the dominant plant photosynthetic pathway despite changing precipitation and temperature (Fig. 5). Palynological records indicate that there were changes in the floristic composition of vegetation, records from Lake Kitandara, another afroalpine lake (3990 m) in the Rwenzori, document a transition from more montane forest species to more alpine taxa (e.g. *Dendrosenecio*) over the last 7 kyr (Livingstone, 1967). Palynological data from Lake Mahoma also indicate substantial changes in vegetation communities, including increased grass during the late Holocene (Livingstone, 1967). Livingstone (1967) interpreted these changes to reflect shifts in local and long-distant pollen transport, or potentially human impacts, though temperature reconstructions from Lake Mahoma suggest the decline in forest taxa may be attributable to cooling (Garelick et al., 2022). Whatever the case may be, our data indicate

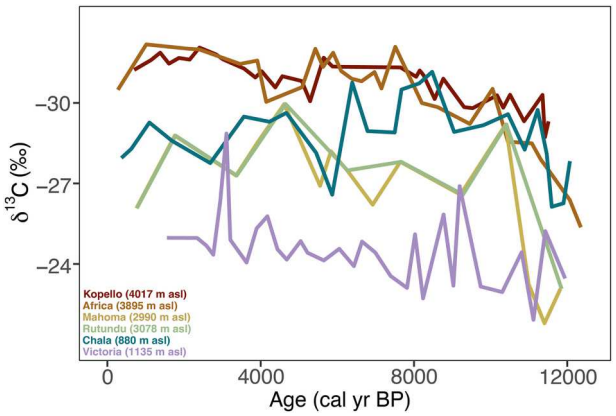

Fig. 5. Rwenzori Mountain $\delta^{13}C_{wax}$ records of the Holocene from Lake Kopello, Lake Africa, and Lake Mahoma (this study), and other $\delta^{13}C_{wax}$ East African records from Lake Rutundu (Wooller et al., 2003), Lake Chala (Sinninghe Damsté et al., 2011), and Lake Victoria (Berke et al., 2012).

these changes, including grass expansion, did not result in a transition to abundant C_4 vegetation. Today, C_4 grasses are nearly completely absent from African mountain ecosystems above 4000 m (Sachse et al., 2012), and our findings indicate that in the Rwenzori this remained the case over the Holocene. This suggests that the combination of atmospheric pCO_2, temperature, and precipitation were sufficient to maintain and favor C_3 vegetation including grasses using the C_3 pathway. This is a reasonable assumption for the Rwenzori Mountains given precipitation totals are greater than other mountains in East Africa thus, minimum precipitation thresholds to trigger transitions to C_4 grasslands may not have been met.

Despite vegetation stability during the Holocene, we observe a brief period of $\delta^{13}C$-enrichment in Lake Africa coincident with the YD at ~11 cal ka BP (Fig. 5). A $\delta^{13}C_{wax}$ record from high-elevation Lake Kimilili (4150 m) on Mt. Elgon, has generally more depleted $\delta^{13}C_{wax}$ than Lake Africa and Lake Kopello, but also shows little variability in $\delta^{13}C_{wax}$ during the Holocene and similar isotope enrichment of C_{31} alkanes associated with the YD (Street-Perrott et al., 1997). Although temperature reconstructions vary, most suggest little to no change during associated with YD in Africa, including the record from Lake Mahoma (Garelick et al., 2022). Our δ^2H_{precip} records suggest that the YD was similar to, and perhaps even less arid than, the late Holocene in the Rwenzori Mountains. These data suggest that the combination of conditions that existed during the YD – slightly lower atmospheric pCO_2, drying, or perhaps disturbance (e.g. fire) – led to an increase in C_4 grasses, and/or increased water stress on high-elevation ecosystems.

In contrast to the afroalpine region, middle-elevation Lake Mahoma does not show the same vegetation stability as the afroalpine sites (Fig. 5). Lake Mahoma undergoes a transition from abundant C_4 vegetation inputs during the YD, to more C_3 vegetation inputs from 11.8 to 10.3 cal ka BP, further confirming the YD interval as a major disruption to montane ecosystems. During the late Holocene, $\delta^{13}C_{wax}$ values also become more enriched coevally with drying indicated by δ^2H, suggesting another expansion of C_4 vegetation, although less pronounced than the YD. Fossil pollen from Lake Mahoma confirms that grasses became more abundant over the late Holocene and YD (Livingstone, 1967), however, given the importance of C_3 bambusoids at the site today, Holocene grass expansion could be partially or largely due to the expansion of mountain bamboo.

Although conditions are generally drier on Mt. Kenya (~1500 mm/yr of precipitation, Ficken et al., 2002), Lake Rutundu (3018 m asl) shows similar $\delta^{13}C_{wax}$ patterns to Lake Mahoma (Fig. 5) (Wooller et al., 2003). However, a pollen record from Lake Rutundu shows no dramatic transitions in major pollen groups over the Holocene (Ficken et al., 2002). Lake Chala also shows variability in $\delta^{13}C_{wax}$ over the Holocene, but less compared to Lake Mahoma and Rutundu (Fig. 6) (Sinninghe Damsté et al., 2011). In Lake Chala, $\delta^{13}C_{wax}$ values are comparatively more depleted during both the YD and middle Holocene. Lake Victoria, in the lowlands, exhibits the most variability in $\delta^{13}C_{wax}$ across the Holocene (Fig. 5). In general, the low-elevation lakes, including sites at middle elevations such as Lakes Mahoma and Rutundu, do not show the same ecosystem stability inferred in the high-elevation lakes. The ecosystem variability in low to mid-elevation ecosystems may be driven by climatic factors such as water stress or other climate thresholds which trigger ecological transitions, human influence, or changing fire regimes which are less prevalent at higher elevations.

5.3. Dynamics of the African Humid Period

Holocene precipitation change in much of Africa is marked by a large transition from wet climates during AHP to a dry late Holocene (Tierney et al., 2011a). Although theory and models agree that seasonal insolation change is the driving mechanism underlying the AHP, there is disagreement on the timing and the abruptness of AHP termination, suggesting regionally variable forcings and/or feedbacks to changing precipitation and seasonal insolation (Tierney and DeMenocal, 2013; Shanahan et al., 2015). Records from northern Africa, such as from the outflow of the Nile and coastal Northwest Africa, indicate an abrupt AHP termination between 7 and 5 cal ka BP, where precipitation declines at a rate much faster than the change in insolation (Castañeda et al., 2016; Tierney et al., 2017), whereas records from further south suggest a more heterogeneous rate of change (Garelick et al., 2021; Berke et al., 2012; Costa et al., 2004; Tierney et al., 2008; Verschuren et al., 2009). The rapid termination in North Africa may be related in part to site-specific responses to gradual migration of the tropical rain belt (Shanahan et al., 2015), nonlinear responses of the monsoon to insolation forcing (DeMenocal et al., 2005), and/or a non-linear response of precipitation to dust and vegetation feedbacks (Tierney et al., 2017; Claussen and Gayler, 1997; Thompson et al., 2019). Although suggestive of abrupt change, it remains difficult to compare the existing records because they rely on a variety of different proxies that have different sensitivities to climate and different response times. Shanahan et al. (2015) compiled a large array of records from different archives and proxies and argued that the AHP termination in Northern Africa was time transgressive, with earlier terminations occurring in the northern most regions. However, syntheses of a more limited number of leaf-wax isotope records have suggested a more synchronized AHP termination (Tierney et al., 2011a).

We synthesized all available leaf wax hydrogen isotope records to examine the dynamics of the AHP termination. We characterize sites based on their location: sites in west Africa are grouped by their influence from the West African Monsoon and sites in east Africa are grouped due to their Indian Ocean influence. These sites include a variety of depositional settings, including offshore marine records, large lakes, and small mountain lakes that sample leaf waxes from very different elevations and catchment areas. This may complicate quantitative comparisons of these datasets due to differences in the isotopic composition of high vs. low-elevation precipitation and smoothing effects from sampling from large catchment areas; however, the geographic patterns of change are not sensitive to any individual record.

Comparisons of sites from the West African Monsoon region show obvious north to south transgressive terminations in which sites furthest north and east (Nile River; Castañeda et al., 2016) shift from wet to dry at ~7 cal ka BP and sites furthest south (Lake Bosumtwi; Shanahan et al., 2015) shift at ~3 cal ka BP (Fig. 6). East African AHP terminations are less straightforward. Many sites show terminations, sometimes rapid, between 6.5 and 4.5 cal ka BP, whereas some δ^2H_{precip} records, such as at Lake Victoria, record a gradual end to the AHP following a precipitation maximum in the early Holocene (~10 ka) (Berke et al., 2012). However, Lake Tanganyika δ^2H_{precip} exhibits an extremely abrupt ending around 5 cal ka BP (Tierney et al., 2008). Records from the Gulf of Guinea and

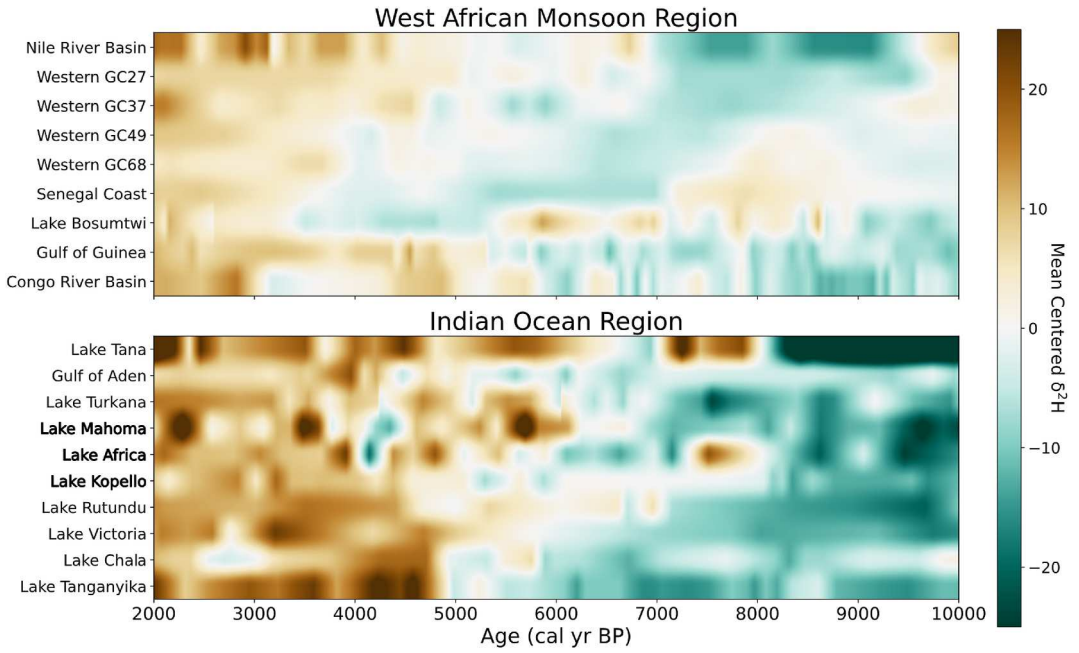

Fig. 6. Holocene mean centered leaf wax δ^2H_{precip} records for sites influenced by the West African Monsoon and sites influenced by Indian Ocean dynamics, organized from north to south for each group. Teal shading indicates depleted δ^2H_{precip} values, or wetter conditions, and brown shading indicates enriched δ^2H_{precip} values, or drier conditions. The sites used are as follows: Nile River (Castañeda et al., 2016), Western GC27 (Tierney et al., 2017), Western GC37 (Tierney et al., 2017), Western GC49 (Tierney et al., 2017), Western GC68 (Tierney et al., 2017), Senegal Coast (Niedermeyer et al., 2010), Lake Bosumtwi (Shanahan et al., 2015), Gulf of Guinea (Collins et al., 2017), Congo River Basin (Schefuβ et al., 2005), Lake Tana (Costa et al., 2004), Gulf of Aden (Tierney and DeMenocal, 2013), Lake Turkana (Morrissey et al., 2014; unpublished), Lake Mahoma (this study), Lake Africa (this study), Lake Kopello (this study), Lake Rutundu (Garelick et al., 2021), Lake Victoria (Berke et al., 2012), Lake Chala (Verschuren et al., 2009), Lake Tanganyika (Tierney et al., 2008).

Congo River Basin, despite their location within the West African monsoon domain, show distinct patterns in δ^2H_{precip} (Fig. 6). Both sites show more variability and earlier AHP termination than west African sites at latitudes directly north. Thus, the data suggest a gradual, time-transgressive termination of the AHP over northwest Africa, but more heterogeneous and, at some sites, abrupt end to the AHP over eastern and equatorial Africa.

Averaging all δ^2H_{precip} records within each region supports our inference that the termination of the AHP was heterogeneous (Fig. 7). The δ^2H_{precip} records in Northwest Africa show, on average, gradual declines from 7 to 4 cal ka BP and more rapid decline thereafter (Fig. 7). In East Africa, precipitation begins to decrease after 9 cal ka BP and declines rapidly until ~4 cal ka BP. Long term trends for central Africa

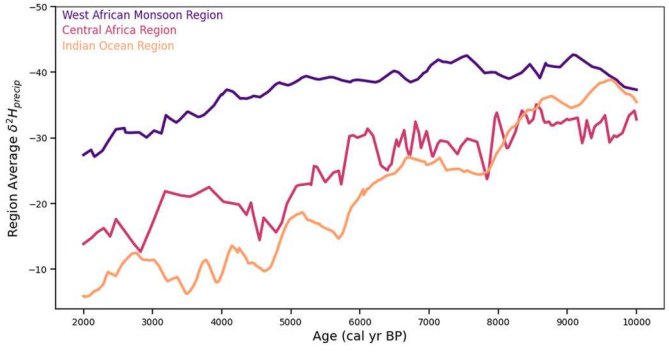

Fig. 7. Leaf wax δ^2H_{precip} record timeseries averaged for each region: West African Monsoon (Nile River Basin, Western GC27, Western GC37, Western GC49, Western GC68, Lake Bosumtwi, Senegal Coast), Central Africa (Congo River Basin, Gulf of Guinea), and Indian Ocean (Lake Africa, Lake Kopello, Lake Mahoma, Lake Tana, Gulf of Aden, Lake Turkana, Lake Rutundu, Lake Victoria, Lake Chala, Lake Tanganyika). Each record was interpolated to a time step of 150 years from 2 to 10 cal ka BP.

are similar to East Africa with a decline starting ~8 cal ka BP and a more rapid decline in precipitation between 6 and 5 cal ka BP.

A primary hypothesis to explain abrupt change in precipitation in North Africa are positive feedbacks between vegetation, surface albedo, and precipitation (Dallmeyer et al., 2020; Renssen et al., 2006). The prolonged interval of high precipitation from ~10 to ~7 cal ka BP, when summer insolation was decreasing, highlights the potential for positive feedbacks that sustained precipitation; however, the gradual changes we observe in δ^2H_{precip} suggest that these feedbacks may be relatively weak. Additionally, climate gradients are much steeper in west Africa compared to eastern Africa, such that latitudinal migration of the monsoon belt can induce abrupt site-specific changes. Eastern and equatorial Africa are less likely to be strongly influenced by vegetation changes because these regions been consistently vegetated through the Holocene. Although plant communities have varied, changes in albedo, latent, and sensible heat are more modest for a transition from moist forest to dry tropical forest than the transition from vegetated landscapes to desert in the Sahara. This suggests that abrupt AHP terminations at ~5 cal ka BP in East Africa likely reflect rapid changes in the atmospheric circulation, such as changes in the position of the CAB. This could influence precipitation as well as changes in the dominant moisture source from the Congo versus the Indian Ocean and thus, cause abrupt δ^2H_{precip} isotope transitions (Berke et al., 2012).

The role of the Indian Ocean and the Congo Air Boundary in East African Holocene precipitation has been widely debated. The Indian Ocean is the primary source of moisture in East Africa and precipitation in the region is sensitive to ITCZ migration, as well as Indian Ocean monsoon dynamics and changes in the Indian Ocean Dipole (Konecky et al., 2014). However, at both Lake Tanganyika and Lake Tana, the role of CAB migration has been posited to explain abrupt rainfall transition during the AHP (Tierney et al., 2008; Costa et al., 2014). The Rwenzori Mountains, located at the interface of the CAB and Indian Ocean, are an ideal location to differentiate between Indian Ocean and CAB influences. Unlike Lake Tanganyika and Lake Tana, our records from the Rwenzori

Mountains do not demonstrate an abrupt δ^2H_{precip} termination at the end of the AHP despite their location between Lake Tana and Lake Tanganyika. Across all three Rwenzori sites, the termination of the AHP begins ~9 cal ka BP and ends gradually until ~4 cal ka BP. These results are consistent with the δ^2H_{precip} records from nearby Lake Rutundu and Lake Victoria which show gradual millennial scale cessation of the AHP (Costa et al., 2014; Tierney et al., 2008). Although AHP dynamics are complex and driven by regional dynamics, it is apparent that time transgressive terminations are an important feature in North Africa. The dynamical drivers are less clear in Central Africa, but in East Africa, the Indian Ocean appears to play a role in AHP dynamics not seen elsewhere.

6. Conclusion

The Rwenzori Mountains experienced dramatic hydroclimate changes over the Holocene. Precipitation changes occurred in response to teleconnections with northern hemisphere climate events such a drying response to AMOC disruption during the Younger Dryas and increased precipitation forced by increased summer insolation. The Rwenzori experienced a gradual end to the AHP, despite its location between regions showing abrupt termination. Despite large precipitation changes, vegetation surrounding high altitude lakes remained dominated by C_3 pants throughout the Holocene. However, mid-elevations experienced ecosystem shifts during the late-Holocene which may have been driven by a decrease in precipitation or other disturbances. Despite complex topography and climatology, the Rwenzori Mountains have responded to regional and northern hemisphere climate changes which resulted in non-uniform ecological change.

CRediT authorship contribution statement

Andrea Mason: Conceptualization, Funding acquisition, Formal analysis, Writing – original draft, Writing – review & editing. **James Russell:** Funding acquisition, Supervision, Conceptualization, Formal analysis, Writing – review & editing. **Sloane Garelick:** Conceptualization, Formal analysis. **Sarah Ivory:** Conceptualization, Writing – review & editing. **Meredith Kelly:** Conceptualization, Writing – review & editing. **Bob Nakileza:** Conceptualization, Writing – review & editing. **Nathan Anderson:** Resources.

Declaration of competing interest

The authors declare that they have no known competing financial interests or personal relationships that could have appeared to influence the work reported in this paper.

Data availability

https://doi.org/10.1594/PANGAEA.972375

Acknowledgements

This research was partially supported by grants from the National Science Foundation (NSF-DEB 2048669) to James Russell. Andrea Mason was partially supported by an NSF Graduate Research Fellowship (NSF-DGE 2040433). We thank Rwenzori Mountaineering Services and Rwenzori Trekking Services for logistical support and helpful guidance in performing fieldwork in the Rwenzori Mountains. Fieldwork and sample export was completed under permits from the Uganda Wildlife Authority (permit #FOD/96/2) and the Uganda National Council for Science and Technology permit number PS-38. We further thank members of the Russell lab and Marcelo Da Rosa Alexandre for laboratory assistance.

Appendix A. Supplementary data

Supplementary data to this article can be found online at https://doi.org/10.1016/j.quascirev.2024.108947.

References

Barker, P.A., Leng, M.J., Greenwood, P.B., Swain, D.L., Perrott, R.A., Telford, R.J., 2001. A 14,000-year oxygen isotope record from diatom silica in two alpine lakes on Mt . Kenya. Science 292, 2307–2310. https://doi.org/10.1126/science.1059612.

Bar-Matthews, M., Ayalon, A., Kaufman, A., Wasserburg, G.J., 1999. The eastern Mediterranean paleoclimate as a reflection of regional events: Soreq Cave, Israel. Earth Planet Sci. Lett. 166 (1–2), 85–95. https://doi.org/10.1016/S0012-821X(98)00275-1.

Berke, M.A., Johnson, T.C., Werne, J.P., Grice, K., Schouten, S., Sinninghe Damsté, J.S., 2012. Molecular records of climate variability and vegetation response since the late pleistocene in the Lake Victoria basin, East Africa. Quat. Sci. Rev. 55, 59–74. https://doi.org/10.1016/j.quascirev.2012.08.014.

Berke, M.A., Johnson, T.C., Werne, J.P., Livingstone, D.A., Grice, K., Schouten, S., Sinninghe Damsté, J.S., 2014. Characterization of the last deglacial transition in tropical East Africa: insights from Lake Albert. Palaeogeogr. Palaeoclimatol. Palaeoecol. 409, 1–8. https://doi.org/10.1016/j.palaeo.2014.04.014.

Bowen, G.J., 2008. Spatial analysis of the intra-annual variation of precipitation isotope ratios and its climatological corollaries. J. Geophys. Res. Atmos. 113, 1–10. https://doi.org/10.1029/2007JD009295.

Bray, E., Evans, E., 1961. Distribution of n-paraffins as a clue to recognition of source beds. Geochem. Cosmochim. Acta 22, 2–15. https://doi.org/10.1016/0016-7037(61)90069-2.

Bwambale, B., Muhumuza, M., Nyeko, M., 2018. Traditional ecological knowledge and flood risk management: a preliminary case study of the Rwenzori. Jamba J. Disaster Risk Stud. 10, 1–10. https://doi.org/10.4102/jamba.v10i1.536.

Castañeda, I.S., Schouten, S., Pätzold, J., Lucassen, F., Kasemann, S., Kuhlmann, H., Schefuß, E., 2016. Hydroclimate variability in the Nile River Basin during the past 28 , 000 years. Earth Planet Sci. Lett. 438, 47–56. https://doi.org/10.1016/j.epsl.2015.12.014.

Cerling, T.E., Wang, Y., Quade, J., 1993. Expansion of C4 ecosystems as an indicator of global ecological change in the late Miocene. Nat 361, 344–345. https://doi.org/10.1038/361344a0.

Claussen, M., Gayler, V., 1997. The greening of the Sahara during the mid-holocene: results of an interactive atmosphere-biome model. Global Ecol. Biogeogr. 6, 369–377. https://doi.org/10.2307/2997337.

Collins, J.A., Prange, M., Caley, T., Gimeno, L., Beckmann, B., Mulitza, S., Skonieczny, C., Roche, D., Schefuß, E., 2017. Rapid termination of the African Humid Period triggered by northern high-latitude cooling. Nat. Commun. 8. https://doi.org/10.1038/s41467-017-01454-y.

Costa, K., Russell, J., Konecky, B., Lamb, H., 2014. Isotopic reconstruction of the African Humid Period and Congo air boundary migration at Lake Tana, Ethiopia. Quat. Sci. Rev. 83, 58–67. https://doi.org/10.1016/j.quascirev.2013.10.031.

Dallmeyer, A., Claussen, M., Lorenz, S.J., Shanahan, T., 2020. The end of the African humid period as seen by a transient comprehensive Earth system model simulation of the last 8000 years. Clim. Past 16, 117–140. https://doi.org/10.5194/cp-16-117-2020.

Dansgaard, W., 1964. Stable isotopes in precipitation. EDIT 2826, 436–468. https://doi.org/10.3402/tellusa.v16i4.8993.

De Menocal, P.B., 2015. Palaeoclimate: end of the African humid period. Nat. Geosci. 8, 86–87. https://doi.org/10.1038/ngeo2355.

De Menocal, P.B., Ortiz, J., Guilderson, T., Adkins, J., Sarnthein, M., Baker, L., Yarusinsky, M., 2000. Abrupt onset and termination of the African Humid Period : rapid climate responses to gradual insolation forcing. Quat. Sci. Rev. 19, 347–361. https://doi.org/10.1016/S0277-3791(99)00081-5.

Diem, J.E., Sung, H.S., Konecky, B.L., Palace, M.W., Salerno, J., Hartter, J., 2019. Rainfall characteristics and trends—and the role of Congo westerlies—in the western Uganda transition zone of equatorial Africa from 1983 to 2017. J. Geophys. Res. Atmos. 124, 10712–10729. https://doi.org/10.1029/2019JD031243.

Doughty, A.M., Kelly, M.A., Russell, J.M., Jackson, M.S., Anderson, B.M., Chipman, J., Nakileza, B.R., 2023. Last glacial maximum reconstructions of Rwenzori mountain glaciers. Paleoceanogr. Paleoclimatol. 38. https://doi.org/10.1029/2022PA004527.

Ehleringer, J.R., Cerling, T.E., Helliker, B.R., 1997. C_4 photosynthesis, atmospheric CO_2, and climate. Oecologica 112, 285–299. https://doi.org/10.1007/s004420050311.

Garelick, S., Russell, J., Richards, A., Smith, J., Kelly, M., Anderson, N., Jackson, M.S., Doughty, A., Nakileza, B., Ivory, S., Dee, S., Marshall, C., 2022. The dynamics of warming during the last deglaciation in high-elevation regions of Eastern Equatorial Africa. Quat. Sci. Rev. 281, 107416. https://doi.org/10.1016/j.quascirev.2022.107416.

Ficken, K.J., Wooller, M.J., Swain, D., Street-Perrott, F.A., Eglinton, G., 2002. Reconstruction of a subalpine grass-dominated ecosystem, Lake Rutundu, Mount Kenya: a novel multi-proxy approach. Palaeogeogr. Palaeoclimatol. Palaeoecol. 177, 137–149. https://doi.org/10.1016/S0031-0182(01)00356-X.

Garelick, S., Russell, J.M., Dee, S., Verschuren, D., Olago, D.O., 2021. Atmospheric controls on precipitation isotopes and hydroclimate in high-elevation regions in Eastern Africa since the Last Glacial Maximum. Earth Planet Sci. Lett. 567, 116984. https://doi.org/10.1016/j.epsl.2021.116984.

Huang, Y., Street-Perrott, F.A.L., Perrott, R.A., Metzger, P., Eglinton, G., 1999. Glacial – interglacial environmental changes inferred from molecular and compound-specific

δ13C analyses of sediments from Sacred Lake, Mt . Kenya. Geochem. Cosmochim. Acta 63, 1383–1404. https://doi.org/10.1016/S0016-7037(99)00074-5.
Karp, A.T., Uno, K.T., Berke, M.A., Russell, J.M., Scholz, C.A., Marlon, J.R., Faith, J.T., Staver, A.C., 2023. Nonlinear rainfall effects on savanna fire activity across the African Humid Period. Quat. Sci. Rev. 304, 107994. https://doi.org/10.1016/j.quascirev.2023.107994.
Kaser, G., Osmaston, H., 2002. Tropical Glaciers. Cambridge University Press.
Konecky, B., Russell, J., Vuille, M., Rehfeld, K., 2014. The Indian Ocean Zonal mode over the past millennium in observed and modeled precipitation isotopes. Quat. Sci. Rev. 103, 1–18. https://doi.org/10.1016/j.quascirev.2014.08.019.
Konecky, B., Russell, J., Bijaksana, S., 2016. Glacial aridity in central Indonesia coeval with intensified monsoon circulation. Earth Planet Sci. Lett. 437, 15–24.
Konecky, B.L., Noone, D.C., Cobb, K.M., 2019. The influence of competing hydroclimate processes on stable isotope ratios in tropical rainfall. Geophys. Res. Lett. 46 (3), 1622–1633. https://doi.org/10.1029/2018GL080188.
Liu, Z., Wang, Y., Gallimore, R., Notaro, M., Prentice, I.C., 2006. On the cause of abrupt vegetation collapse in North Africa during the Holocene: climate variability vs. vegetation feedback. Geophys. Res. Lett. 33. https://doi.org/10.1029/2006GL028062.
Liu, Z., Bao, Y., Thompson, L.G., Mosley-Thompson, E., Tabor, C., Zhang, G.J., Yan, M., Lofverstrom, M., Montanez, I., Oster, J., 2023. Tropical mountain ice core δ18O: a Goldilocks indicator for global temperature change. Sci. Adv. 9. https://doi.org/10.1126/sciadv.adi6725.
Livingstone, D.A., Clayton, W.D., 1980. An altitudinal cline in tropical african grass floras and its paleoecological significance. Quat. Res. 13, 392–402. https://doi.org/10.1016/0033-5894(80)90065-4.
Livingstone, D.A., 1967. Postglacial vegetation of the ruwenzori mountains in equatorial Africa. Ecol. Monogr. 37, 25–52. https://doi.org/10.2307/1948481.
McKay, N.P., Emile-Geay, J., Khider, D., 2021. geoChronR – an R package to model, analyze, and visualize age-uncertain data. Geochronology 3, 149–169. https://doi.org/10.5194/gchron-3-149-2021.
Mitsunaga, B.A., Lupien, R.L., Ouertani, S., Stubbs, B., Deino, A.L., Kingston, J.D., Stockhecke, M., Brown, E.T., Russell, J.M., 2023. High-latitude, Indian Ocean, and orbital influences on Eastern African hydroclimate across the plio-pleistocene boundary. Paleoceanogr. Paleoclimatol. 38. https://doi.org/10.1029/2023PA004671.
Niang, O. Ruppel, Abdrabo, M., Essel, A., Lennard, C., Padgham, J., Urquhart, P., 2014. Africa Climate Change 2014: Impacts, Adaptation, and Vulnerability. Part B: Regional Aspects Contribution of Working Group II to the Fifth Assessment Report of the Intergovernmental Panel on Climate Change. Cambridge Univ Press, Cambridge, UK. https://doi.org/10.1017/CBO9781107415386.
Nicholson, S.E., 2017. Climate and climatic variability of rainfall over eastern Africa. Rev. Geophys. 55, 590–635. https://doi.org/10.1002/2016RG000544.
Niedermeyer, E.M., Schefuß, E., Sessions, A.L., Mulitza, S., Mollenhauer, G., Schulz, M., Wefer, G., 2010. Orbital- and millennial-scale changes in the hydrologic cycle and vegetation in the western African Sahel : insights from individual plant wax dD and d13C. Quat. Sci. Rev. 29, 2996–3005. https://doi.org/10.1016/j.quascirev.2010.06.039.
Osmaston, H.A., 1989. Glaciers, glaciations, and equilibrium line altitudes on the Ruwenzori. Quat. Environ. Res. East Afr. Mt. 1, 31–104. https://doi.org/10.1201/9781003211457-3.
Otto-Bliesner, B.L., Russell, J.M., Clark, P.U., Overpeck, J.T., Konecky, B., Demenocal, P., Nicholson, E., He, F., Lu, Z., 2014. Coherent changes of southeastern equatorial and northern African rainfall during the last deglaciation. Science 346, 1223–1227. https://doi.org/10.1126/science.1259531.
Oyana, T., Nakileza, B.R., 2016. Assesssing adaptability and response of vegetation to glacier recesssion in the afro-alpine moorland terrestrial ecosystem of Rwenzori Mountains. J. Mt. Sci. 13, 1584–1597. https://doi.org/10.1007/s11629-015-3504-z.
Renssen, H., Brovkin, V., Fichefet, T., Goosse, H., 2006. Simulation of the holocene climate evolution in Northern Africa: the termination of the African humid period. Quat. Int. 150, 95–102. https://doi.org/10.1016/j.quaint.2005.01.001.
Rowley, D.B., Garzione, C.N., 2007. Stable isotope-based paleoaltimetry. Annu. Rev. Earth Planet Sci. 35, 463–508. https://doi.org/10.1146/annurev.earth.35.031306.140155.
Russell, J., Eggermont, H., Taylor, R., Verschuren, D., 2009. Paleolimnological records of recent glacier recession in the Rwenzori Mountains, Uganda-D. R. Congo. J. Paleolimnol. 41, 253–271. https://doi.org/10.1007/s10933-008-9224-4.
Russell, J.M., Johnson, T.C., Kelts, K.R., Lærdal, T., Talbot, M.R., 2003. An 11 000-year lithostratigraphic and paleohydrologic record from equatorial Africa: lake Edward, Uganda-Congo. Palaeogeogr. Palaeoclimatol. Palaeoecol. 193, 25–49. https://doi.org/10.1016/S0031-0182(02)00709-5.
Sachse, D., Billault, I., Bowen, G.J., Chikaraishi, Y., Dawson, T.E., Feakins, S.J., Freeman, K.H., Magill, C.R., McInerney, F.A., Van Der Meer, M.T.J., Polissar, P., Robins, R.J., Sachs, J.P., Schmidt, H.L., Sessions, A.L., White, J.W.C., West, J.B., Kahmen, A., 2012. Molecular paleohydrology: interpreting the hydrogen-isotopic composition of lipid biomarkers from photosynthesizing organisms. Annu. Rev. Earth Planet Sci. 40, 221–249. https://doi.org/10.1146/annurev-earth-042711-105535.
Schefuß, E., Schouten, S., Schneider, R.R., 2005. Climatic controls on central African hydrology during the past 20,000 years. Nat 437, 1003–1006. https://doi.org/10.1038/nature03945.
Schnurrenberger, D., Russell, J., Kelts, K., 2003. Classification of lacustrine sediments based on sedimentary components. J. Paleolimnol. 29, 141–154. https://doi.org/10.1023/A:1023270324800.
Sessions, A.L., Burgoyne, T.W., Hayes, J.M., 2001. Determination of the H_3 factor in hydrogen isotope ratio monitoring mass spectrometry. Anal. Chem. 73, 200–207. https://doi.org/10.1021/ac000488m.
Shanahan, T.M., Mckay, N.P., Hughen, K.A., Overpeck, J.T., Otto-Bliesner, B., Heil, C.W., King, J., Scholz, C.A., Peck, J., 2015. The time-transgressive termination of the African humid period. Nat. Geosci. 8, 140–144. https://doi.org/10.1038/ngeo2329.
Sinninghe Damsté, J.S., Verschuren, D., Ossebaar, J., Blokker, J., van Houten, R., van der Meer, M.T.J., Plessen, B., Schouten, S., 2011. A 25,000-year record of climate-induced changes in lowland vegetation of eastern equatorial Africa revealed by the stable carbon-isotopic composition of fossil plant leaf waxes. Earth Planet Sci. Lett. 302, 236–246. https://doi.org/10.1016/j.epsl.2010.12.025.
Street-Perrott, F.A., Barker, P.A., Swain, D.L., Ficken, K.J., Wooller, M.J., Olago, D.O., Huang, Y., 2007. Late Quaternary changes in ecosystems and carbon cycling on Mt . Kenya , East Africa : a landscape-ecological perspective based on multi-proxy lake-sediment influxes. Quat. Sci. Rev. 26, 1838–1860. https://doi.org/10.1016/j.quascirev.2007.02.014.
Street-Perrott, F.A., Huang, Y., Perrott, R.A., Eglinton, G., Barker, P., Ben Khelifa, L., Harkness, D.D., Olago, D.O., 1997. Impact of lower atmospheric carbon dioxide on tropical mountain ecosystems. Science 278, 1422–1426. https://doi.org/10.1126/science.278.5342.1422.
Stuiver, M., Reimer, P.J., 1993. Radiocarbon 35, 215–230.
Taylor, R.G., Mileham, L., Tindimugaya, C., Mwebembezi, L., 2009. Recent glacial recession and its impact on alpine riverflow in the Rwenzori Mountains of Uganda. J. African Earth Sci. 55, 205–213. https://doi.org/10.1016/j.jafrearsci.2009.04.008.
Thompson, A.J., Skinner, C.B., Poulsen, C.J., Zhu, J., 2019. Modulation of mid-holocene African rainfall by dust aerosol direct and indirect effects. Geophys. Res. Lett. 46, 3917–3926. https://doi.org/10.1029/2018GL081225.
Thompson, L.G., Mosley-thompson, E., Davis, M.E., Henderson, K.A., Brecher, H.H., Zagorodnov, V.S., Mashiotta, T.A., Lin, P., Mikhalenko, V.N., Hardy, D.R., 2002. Kilimanjaro ice core records : evidence of holocene climate change in tropical Africa. Science 298, 589–593.
Tierney, J.E., DeMenocal, P.B., 2013. Abrupt shifts in Horn of Africa hydroclimate since the last glacial maximum. Science 342, 843–846. https://doi.org/10.1126/science.1240411.
Tierney, J.E., Lewis, S.C., Cook, B.I., LeGrande, A.N., Schmidt, G.A., 2011a. Model, proxy and isotopic perspectives on the East African Humid Period. Earth Planet Sci. Lett. 307, 103–112. https://doi.org/10.1016/j.epsl.2011.04.038.
Tierney, J.E., Pausata, F.S.R., De Menocal, P.B., 2017. Rainfall regimes of the green Sahara. Sci. Adv. 3, 1–10. https://doi.org/10.1126/sciadv.1601503.
Tierney, J.E., Russell, J.M., Huang, Y., Sinninghe Damsté, J.S., Hopmans, E.C., Cohen, A. S., 2008. Northern hemisphere controls on tropical southeast African climate during the past 60,000 years. Science 322, 252–255. https://doi.org/10.1126/science.1160485.
Tierney, J.E., Russell, J.M., Sinninghe Damsté, J.S., Huang, Y., Verschuren, D., 2011b. Late quaternary behavior of the East African monsoon and the importance of the Congo air boundary. Quat. Sci. Rev. 30, 798–807. https://doi.org/10.1016/j.quascirev.2011.01.017.
Trisos, C.H., Adelekan, I.O., Totin, E., Ayanlade, A., Efitre, J., Gemeda, A., Kalaba, K., Lennard, C., Masao, C., Mgaya, Y., Ngaruiya, G., Olago, D., Simpson, N.P., Zakieldeen, S., 2022. Africa. In: Climate Change 2022: Impacts, Adaptation, and Vulnerability. Contribution of Working Group II to the Sixth Assessment Report of the Intergovernmental Panel on Climate Change. IPCC. https://doi.org/10.1017/9781009325844.011.1286.
Uno, K.T., Polissar, P.J., Kahle, E., Feibel, C., Harmand, S., Roche, H., deMenocal, P.B., 2016. A Pleistocene palaeovegetation record from plant wax biomarkers from the Nachukui Formation, West Turkana, Kenya. Philos. Trans. R. Soc. Lond. B Biol. Sci. 371, 20150235. https://doi.org/10.1098/rstb.2015.0235.
Van Vooren, S., Van Schaeybroeck, B., Nyssen, J., Van Ginderachter, M., Termonia, P., 2019. Evaluation of CORDEX rainfall in northwest Ethiopia: sensitivity to the model representation of the orography. Int. J. Climatol. 39, 2569–2586. https://doi.org/10.1002/joc.5971.
Verschuren, D., Sinninghe Damsté, J.S., Moernaut, J., Kristen, I., Blaauw, M., Fagot, M., Haug, G.H., 2009. Half-precessional dynamics of monsoon rainfall near the East African Equator. Nat 462, 637–641. https://doi.org/10.1038/nature08520.
Wooller, M.J., Swain, D.L., Ficken, K.J., Agnew, A.D.Q., Street-Perrott, F.A., Eglinton, G., 2003. Late Quaternary vegetation changes around Lake Rutundu, Mount Kenya, East Africa: evidence from grass cuticles, pollen and stable carbon isotopes. J. Quat. Sci. 18, 3–15. https://doi.org/10.1002/jqs.725.